ARO 16873.5-PH

FINAL REPORT

MILLIMETER AND SUBMILLIMETER WAVE RESEARCH:

SPECTROSCOPY, ENERGY TRANSFER, AND TECHNIQUES

Frank C. De Lucia

January 16, 1984

Department of Physics

Duke University

Durham, North Carolina 27706

AD A137884

DTIC FILE COPY

DTIC
ELECTE
FEB 1 5 1984

S

A

84   02   14   101

1. REPORT NUMBER	2. GOVT ACCESSION NO.	3. RECIPIENT'S CATALOG NUMBER
Final Report	AD-A137884	

4. TITLE (and Subtitle)	5. TYPE OF REPORT & PERIOD COVERED
Millimeter and Submillimeter Wave Research: Spectroscopy, Energy Transfer, and Techniques	Final Report 5 Nov 79 – 5 Nov 83
	6. PERFORMING ORG. REPORT NUMBER
	Duke U. Dept. of Physics

7. AUTHOR(s)	8. CONTRACT OR GRANT NUMBER(s)
Frank C. De Lucia	DAAG-29-83-K-0028 80-C-0026

9. PERFORMING ORGANIZATION NAME AND ADDRESS	10. PROGRAM ELEMENT, PROJECT, TASK AREA & WORK UNIT NUMBERS
Department of Physics Duke University Durham, North Carolina	

11. CONTROLLING OFFICE NAME AND ADDRESS	12. REPORT DATE
U. S. Army Research Office P. O. Box 12211 Research Triangle Park, NC 27709	January 16, 1984
	13. NUMBER OF PAGES
	approx. 34

14. MONITORING AGENCY NAME & ADDRESS(if different from Controlling Office)	15. SECURITY CLASS. (of this report)
	Unclassified
	15a. DECLASSIFICATION/DOWNGRADING SCHEDULE

16. DISTRIBUTION STATEMENT (of this Report)

Approved for public release; distribution unlimited.

17. DISTRIBUTION STATEMENT (of the abstract entered in Block 20, if different from Report)

18. SUPPLEMENTARY NOTES

The view, opinions, and/or findings contained in this report are those of the author(s) and should not be construed as an official Department of the Army position, policy, or decision, unless so designated by other documentation.

19. KEY WORDS (Continue on reverse side if necessary and identify by block number)

Millimeter Waves	Molecular Lasers
Submillimeter Waves	Molecular Energy Levels
Spectroscopy	
Energy Transfer	

20. ABSTRACT (Continue on reverse side if necessary and identify by block number)

The project, "Millimeter and Submillimeter Wave Research: Spectroscopy, Energy Transfer, and Techniques," addresses a broad range of scientific topics and technological developments important to this spectral region. For purposes of discussion, we have divided this report into three categories: (1) the development and evolution of techniques for this spectral region, (2) studies of molecular lasers and processes, and (3) the study of energy levels and transition frequencies in molecules. Also included are lists of publications and of personnel who worked on these projects.

DD FORM 1473   EDITION OF 1 NOV 65 IS OBSOLETE

Unclassified

SUMMARY OF WORK UNDER ARO CONTRACT DAAG-29-83-K-0078

The project, "Millimeter and Submillimeter Wave Research:
Spectroscopy, Energy Transfer, and Techniques," addresses a broad
range of scientific topics and technological developments impor-
tant to this spectral region. For purposes of discussion, ~~we~~ this
report have divided ~~this report~~ into three categories:
(1) the development and evolution of techniques for this spectral
region, (2) studies of molecular lasers and processes, and (3) the
study of energy levels and transition frequencies in molecules.
Also included are lists of publications and of personnel who
worked on these projects.

I. Experimental Techniques and Devices

We have extended our basic source technique to beyond 1 THz
so that now the entire NMMW spectral region (100 GHz-1000 GHz)
can be covered. This advance came about primarily as a result of
a redesign of our non-linear harmonic generators. Figure 1 shows
an example of a basic system configured around this source. Simple
changes would result in a system appropriate for component studies,
detector development, etc.

This technique has a number of favorable attributes:

(1) It is continuously tunable throughout the spectral region,
<100 GHz->1000 GHz.

(2) Systems based on the harmonics of phase locked klystrons
have resolution limited only by the physical processes being
studied. Furthermore, they have absolute frequency calibration
by direct reference to WWVB.

(3) Although the amount of power produced by harmonic genera-
tion is modest, the systematic increase ($\sim v^3$) of the strength of
rotational transitions with frequency and our use of cryogenic
detection techniques result in a very high sensitivity technique.

(4) The MM/SUBMM lends itself to quasi-optical techniques.
These techniques make possible the remote sampling of hostile
environments, pressure broadening cells, etc. without affecting
the system under study.

(5) It is simple, reliable, and reasonably inexpensive. A
number of systems patterned on this design have been built at
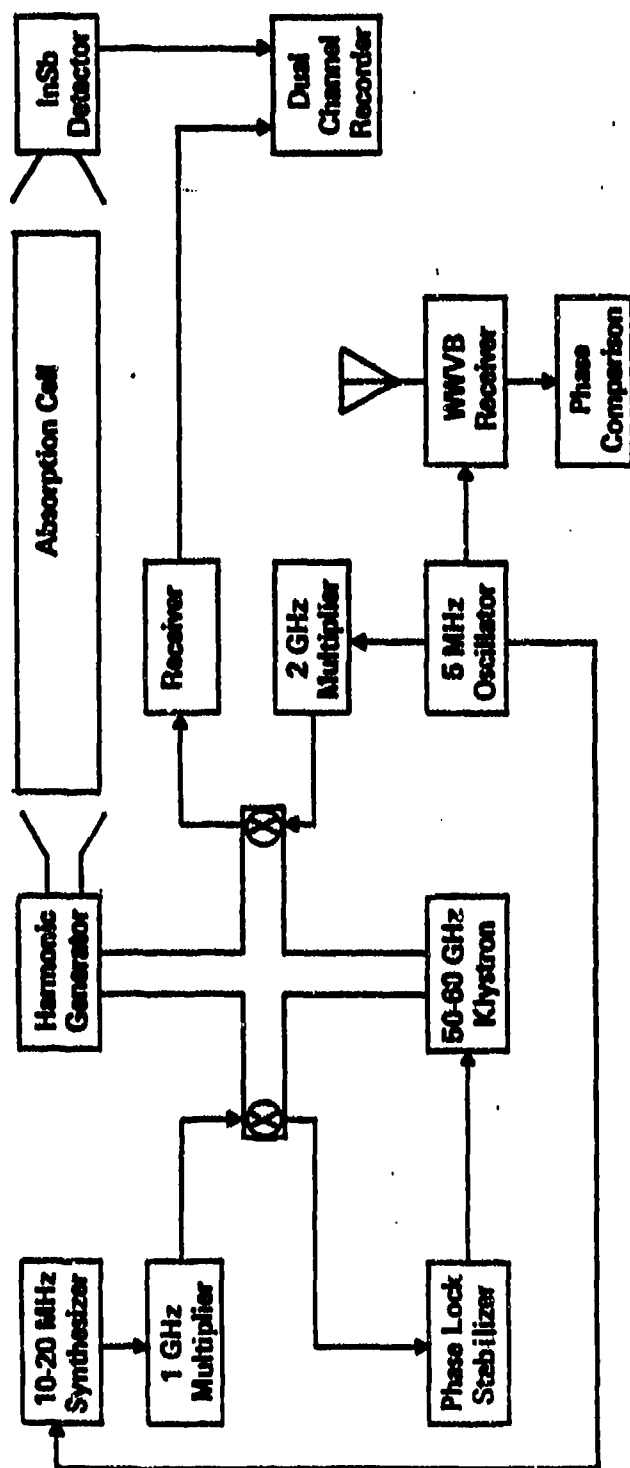leading government and university laboratories throughout the
world.

Figure 1. Basic system for work throughout the NMMW spectral region (<100->1000 GHz). Configuration shown is for absorption studies of gases.

For our studies of optically pumped FIR lasers, we have developed the experimental apparatus shown in Figure 2. Briefly, this system consists of a line tunable CO_2 laser, tunable MM/SUBMM spectrometer, and a FIR gain cell in which the CO_2 laser beam and microwave diagnostic beam copropagate. In order to minimize errors induced by long term drifts and to make possible absolute rather than relative experimental results, the CO_2 laser is chopped at ~15 Hz. The data recorded in the absence of the pump, in combination with the well know relations for the absorption coefficients of gases in thermal equilibrium, provide an absolute calibration for our work. This procedure is feasible because the sensitivity of our techniques allows us to observe the absorptions with good signal to noise even in excited vibrational states. This system has made it possible to realistically model for the first time the energy transfer processes in optically pumped FIR lasers. A similar system has been developed for our studies of discharge laser systems.

We have also developed new techniques that have increased the detectability of molecular ions in the NMMW by three orders of magnitude. This is an especially significant fundamental develop-ment. Briefly, we use an axial magnetic field to lengthen the ion rich negative glow of an abnormal glow discharge. Figure 3 shows the cell and Figure 4 shows the dramatic effect of this. This tech-nique is being currently adopted by the other workers in this field.
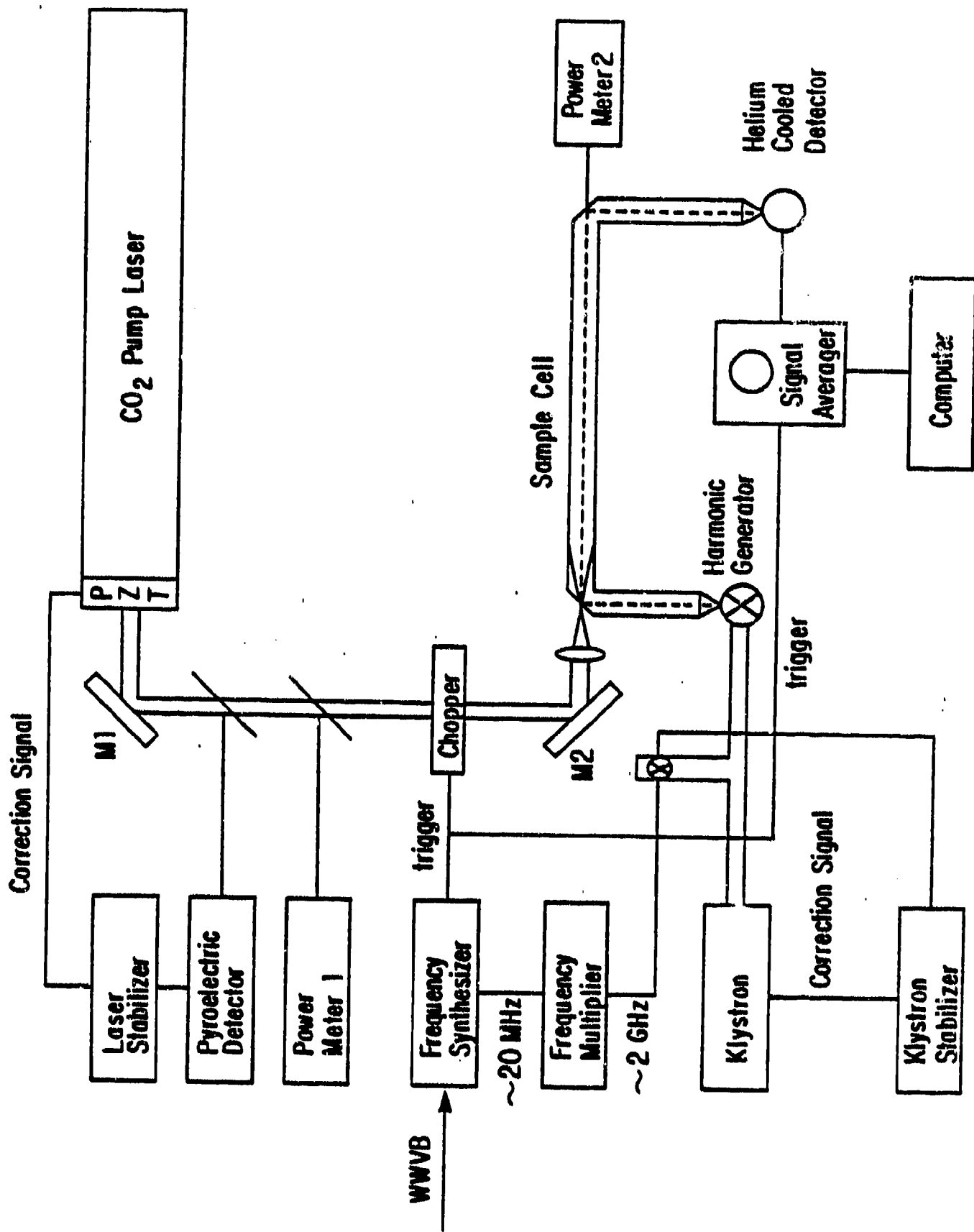
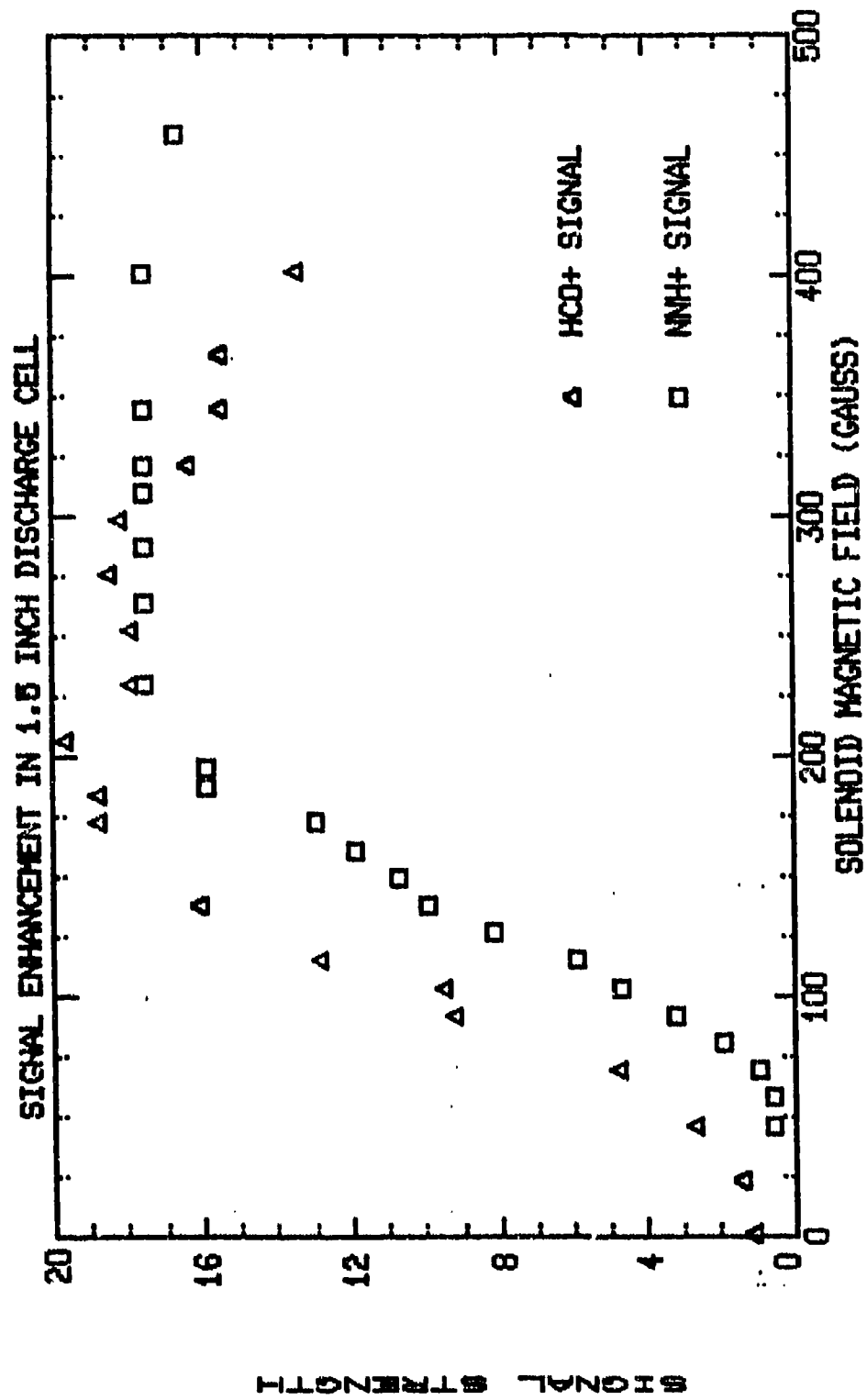Figure 2. Spectrometer for the study of optically pumped laser systems.

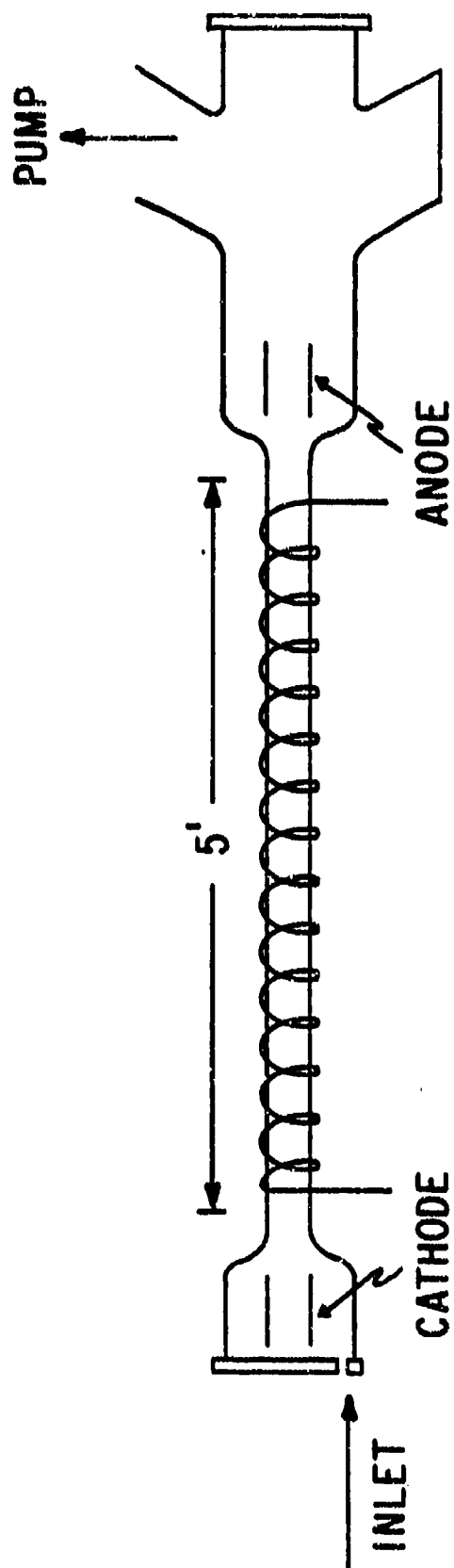Figure 4a. Signal enhancement with the application of magnetic field.

Figure 3. Cell for new magnetic confinement technique for the study of molecular ions.
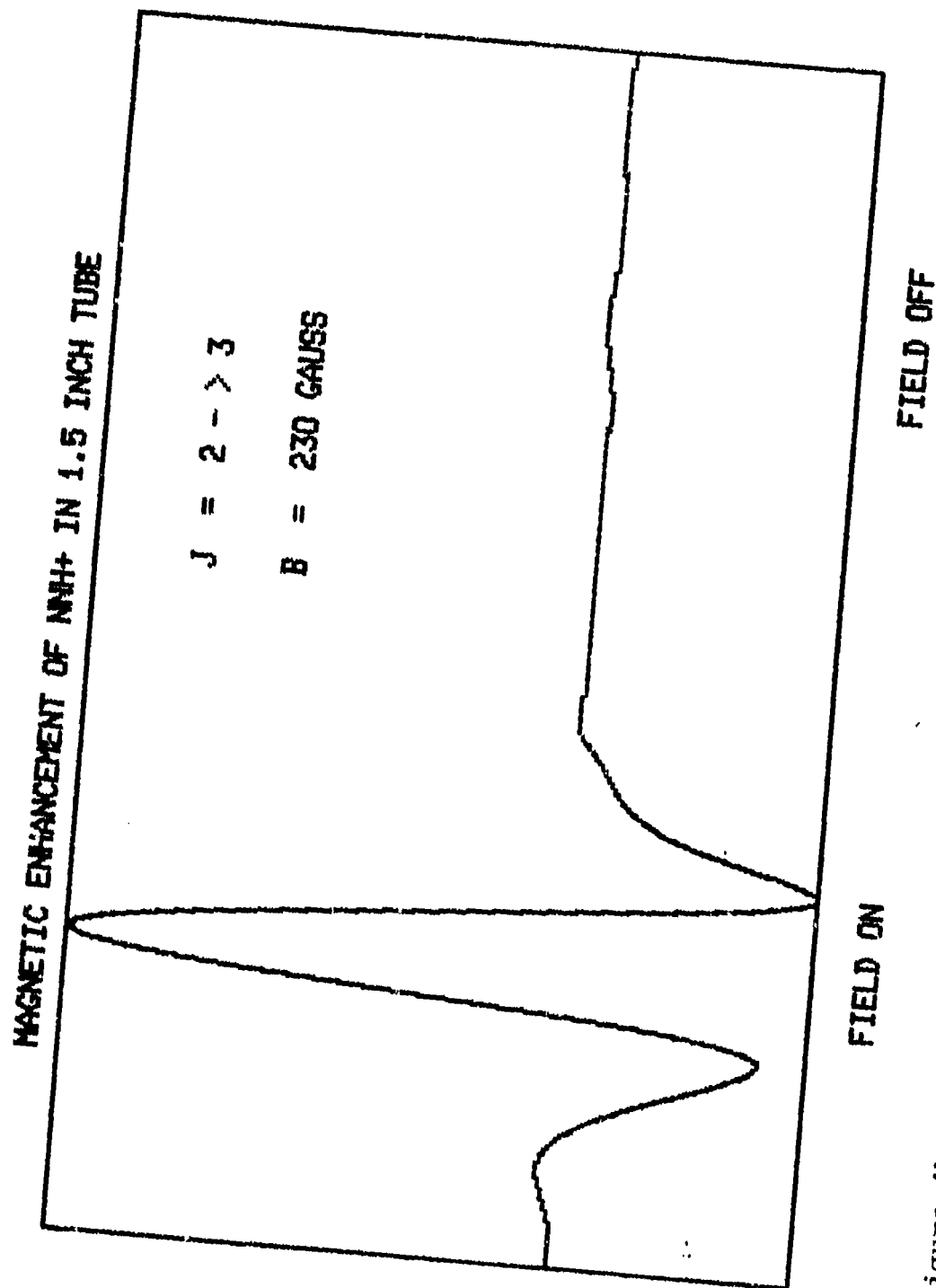
MAGNETIC ENHANCEMENT OF NNH+ IN 1.5 INCH TUBE

$J = 2 -> 3$

$B = 230$ GAUSS

FIELD ON

FIELD OFF

Figure 4b. Effect of magnetic field on signal.

II. Studies of Molecular Lasers and Processes

We have used the system shown in Figure 2 to study the energy transfer processes in optically pumped FIR processes.

Figure 5 shows a pair (pumped/unpumped) of observations for the ν_3, J=4-5, K=3,2,1, and 0 transitions of $^{13}CH_3F$. This figure shows the dramatic effect of the CO_2 pump on the ν_3, J=5, K=3 level. Of equal, or perhaps greater importance, is the information given on the K≠3 levels. Careful inspection of these (and all other ν_3, K≠3 levels) show them to have an enhanced absorption and to be in thermal equilibrium with one another. In order to account for these data and data on many other transitions that our continuously tunable technique has allowed us to obtain , we have developed the energy transfer model shown in Figure 6. In this model the experimentally observed rotational thermal equilibrium is implemented via a ground state (K≠3) pool and an excited state (K≠3) pool. We observe substantial deviations from thermal equilibrium within K=3 and the population of each of these states (up to J=42) is allowed to vary independently. The states/pools are allowed to exchange populations via the pump rate (R), the probability of ΔJ=±1, ΔK=0 collisional tranfers (P_{up}/P_{down}), the probability of collisional exchange between the K=3 states and their respective pools (P_{in}/P_{out}), and the probability of collisional exchange between the vibrational pools (PV_{up}/PV_{down}). Because these probabilities must obey microscopic reversibility and because one of them must be fixed to define a collision, this system has only three adjustable parameters. In our analysis, we recorded data at 7 pressures and used a non-linear
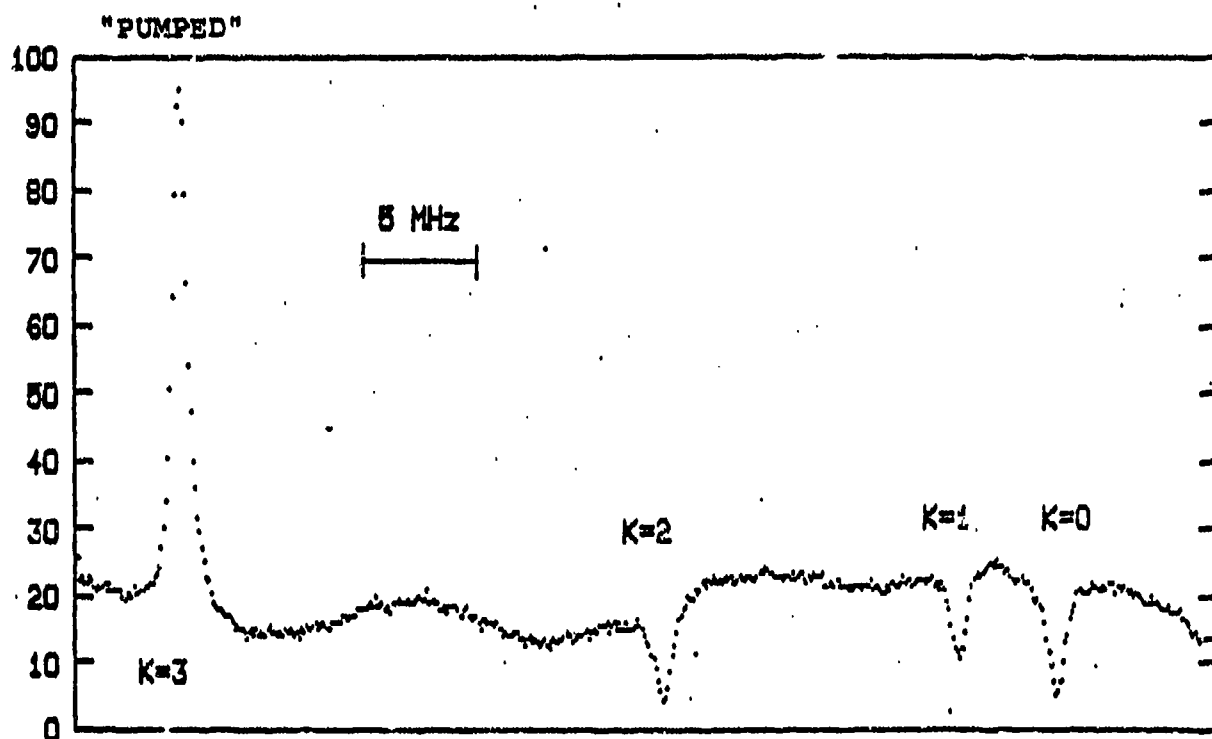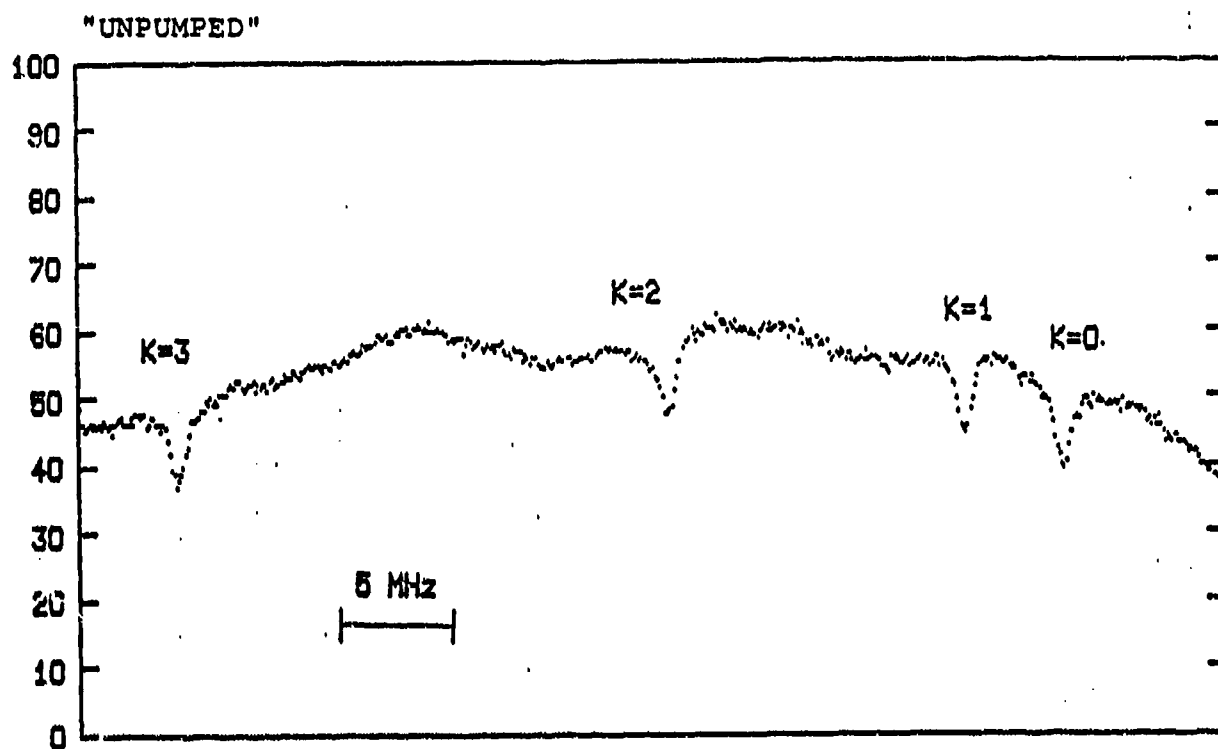
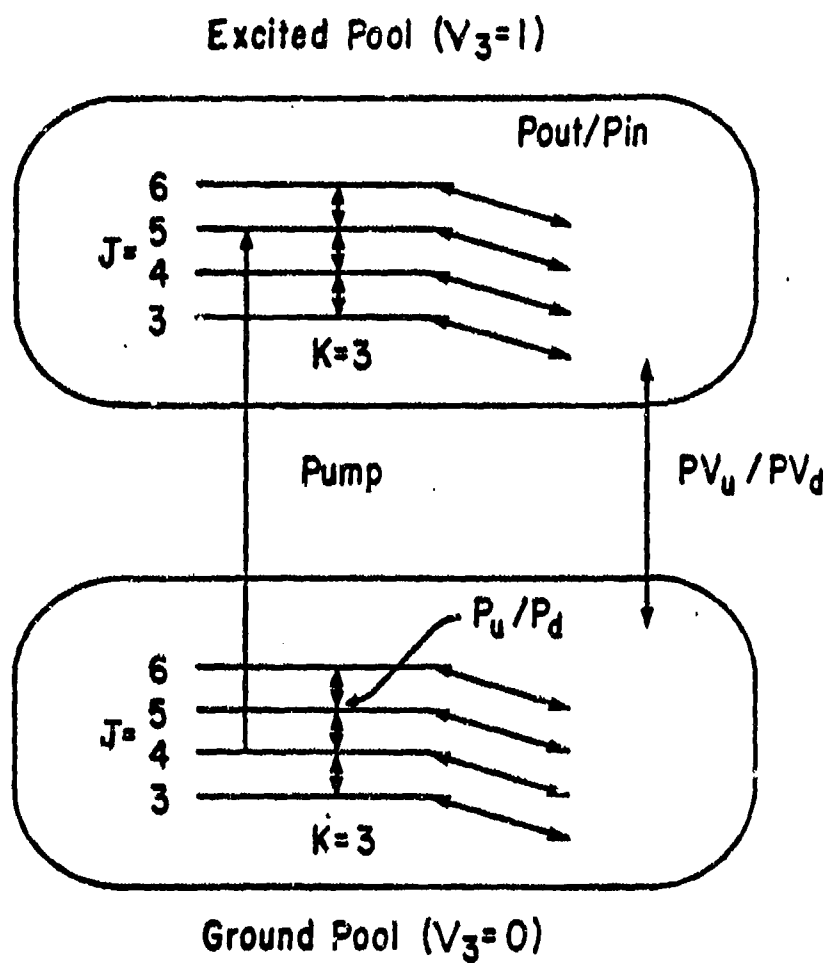Figure 5. Effect of CO_2 laser pumping on the ν_3, J=4-5, K=3,2,1, and 0 transitions of $^{13}CH_3F$.

Figure 6. Schematic of energy transfer model for the $^{13}CH_3F$ optically pumped laser.

least squares implementation of a master equation to calculate these probabilities and transition rates. Figure 7 shows the results of these seven fits for the pump rate [photons/(sec-cm^3)]. In the absence of saturation, this curve should be a horizontal line. However, an inhomogeneously broadened line should have a saturation factor of $1/\sqrt{1+I_v/I_s}$, which is included in our best fit line. Although the pump rates shown in this figure were deduced from our spectroscopic data and theoretical model, we have also made a direct measurement of the laser power absorbed. This measurement gives a number about 20% higher than the spectroscopically deduced value. This is an excellent agreement between two very different (and in one case model dependent) observations. Figure 8 shows a similar result for $1/PV_d$. Our experiments have demonstrated the necessity of distinguishing between "hard" velocity changing collisions and "soft" collisions that induce rotational transitions but which do not appreciably affect the molecular trajectories. This is especially important in energy transfer models of the $^{13}CH_3F$ laser. The collisions that induce $\Delta J=\pm 1$, $\Delta K=0$ transitions are ~x20 more likely than the "hard" collisions that lead to random walk processes. Figure 8 also includes a straight line. This line represents a value of $1/PV_d$ calculated for straight line molecular trajectories to the wall (i.e. no random walk) and vibrational equilibriation upon wall collision. This line and our experimental results are again very consistent with our calculation that only ~1-2 hard collisions occur along the trajectory of a molecule to the wall at 10 μ. This small
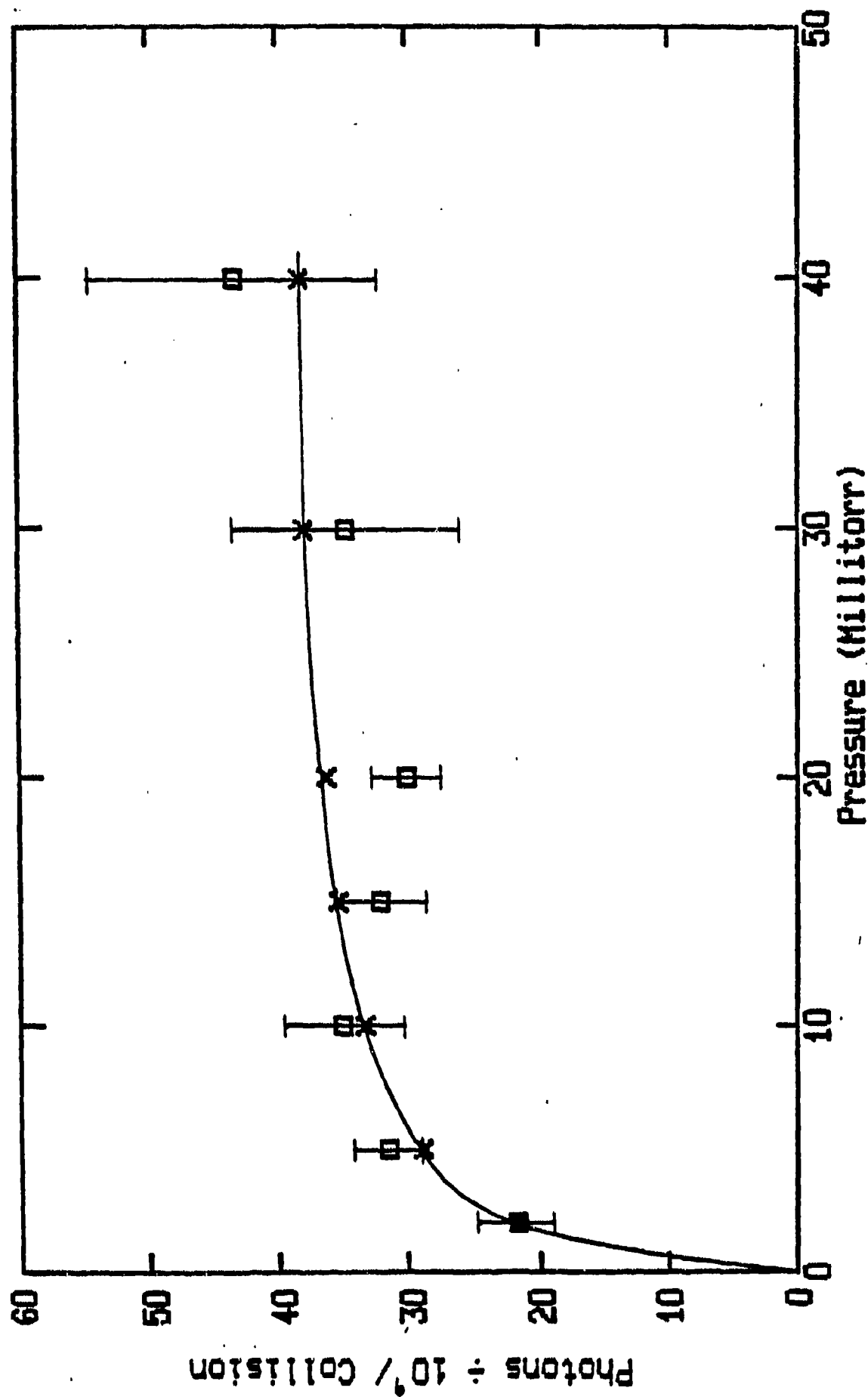
Figure 7. Pump rate of the $^{13}CH_3F$ optically pumped laser. □'s are results from least squares fit to spectroscopic data. X's are points on best fit line.

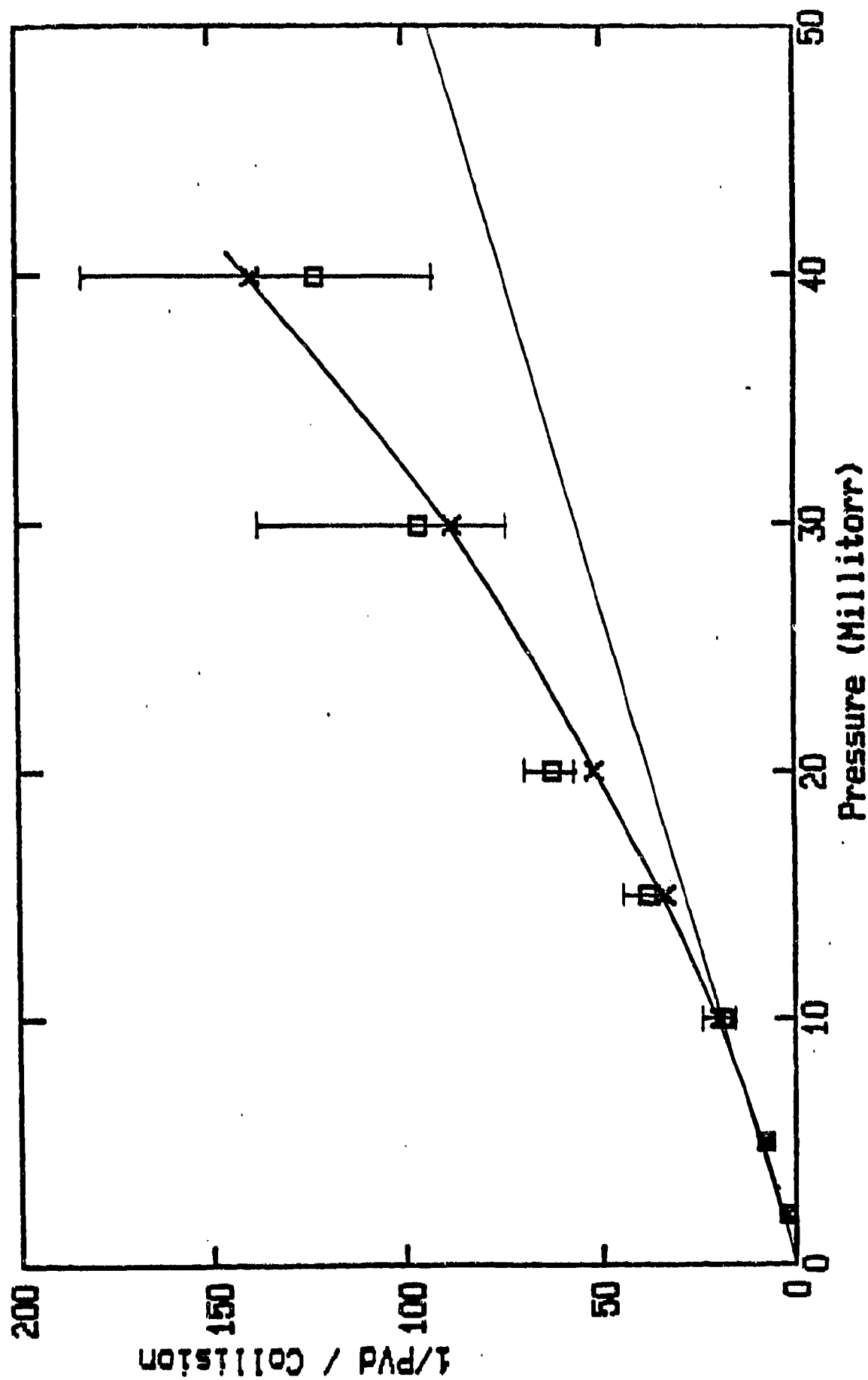Figure 8. Reciprocal of the vibrational decay probability of the $^{13}CH_3F$ optically pumped laser. □'s are results from least squares fit to spectroscopic data. X's are points on best fit line.
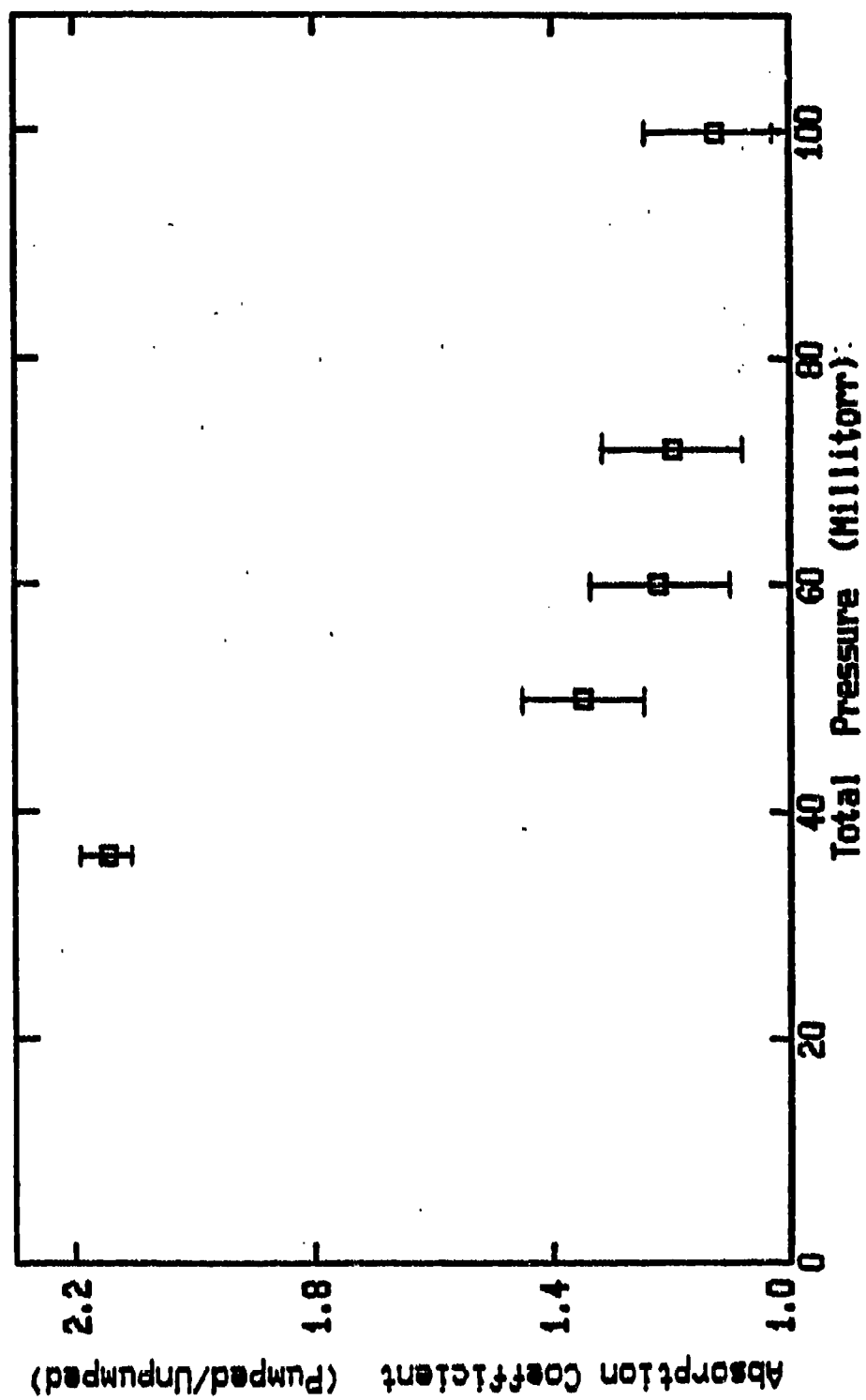
Figure 9. Ratio of pumped/unpumped absorption coefficient for the $V_3 = 1$, $J=4->5$, $K=2$ transition in the 2" cell with hexane

random walk effect is a direct cause of the relatively small $K \neq 3$ vibrational enhancement seen in Figure 5. A similar plot can be shown for P_{in}/P_{out}, but its interpretation in terms of a vibrationally resonant exchange process is too lengthy to discuss here.

We have also studied the effects of the addition of foreign buffer gases on the operation of optically pumped FIR lasers. An example of the kinds of results obtained in this experiment is shown in Figure 9. The absorption of this transition is a direct measure of vibrational bottlenecking in optically pumped lasers. In pure $^{13}CH_3F$ 10,000 collisions are required to deactivate the $v_3=1$ excited vibrational state. From the data shown in this figure, it can be calculated that only 5 collisions with Hexane are required. We have done similar studies with Helium. Figure 10 shows a result calculated from our model. This graph, which is a function of the addition of hexane, shows the change in transtion probability between collisions which force $\Delta J = \pm 1$ equilibriating transitions and ΔK transitions which empty the lasing stack.

We have used the system shown in Figure 11 to study the HCN FIR discharge laser and vibrational and rotational processes in the OCS system. Figure 12 shows the $J=2-3$ rotational transitions of the 100, 11^10, 001, and 01^11 states of HCN. This is a fortuitious conjunction that allows simultaneous observation of these states under identical discharge conditions. A detailed comparison of the $100/11^10$ and $001/01^11$ pairs show that the bending modes are in thermal equilibrium (at the rotational/translational temperature of the discharge) with their stretching parent mode. However, as shown
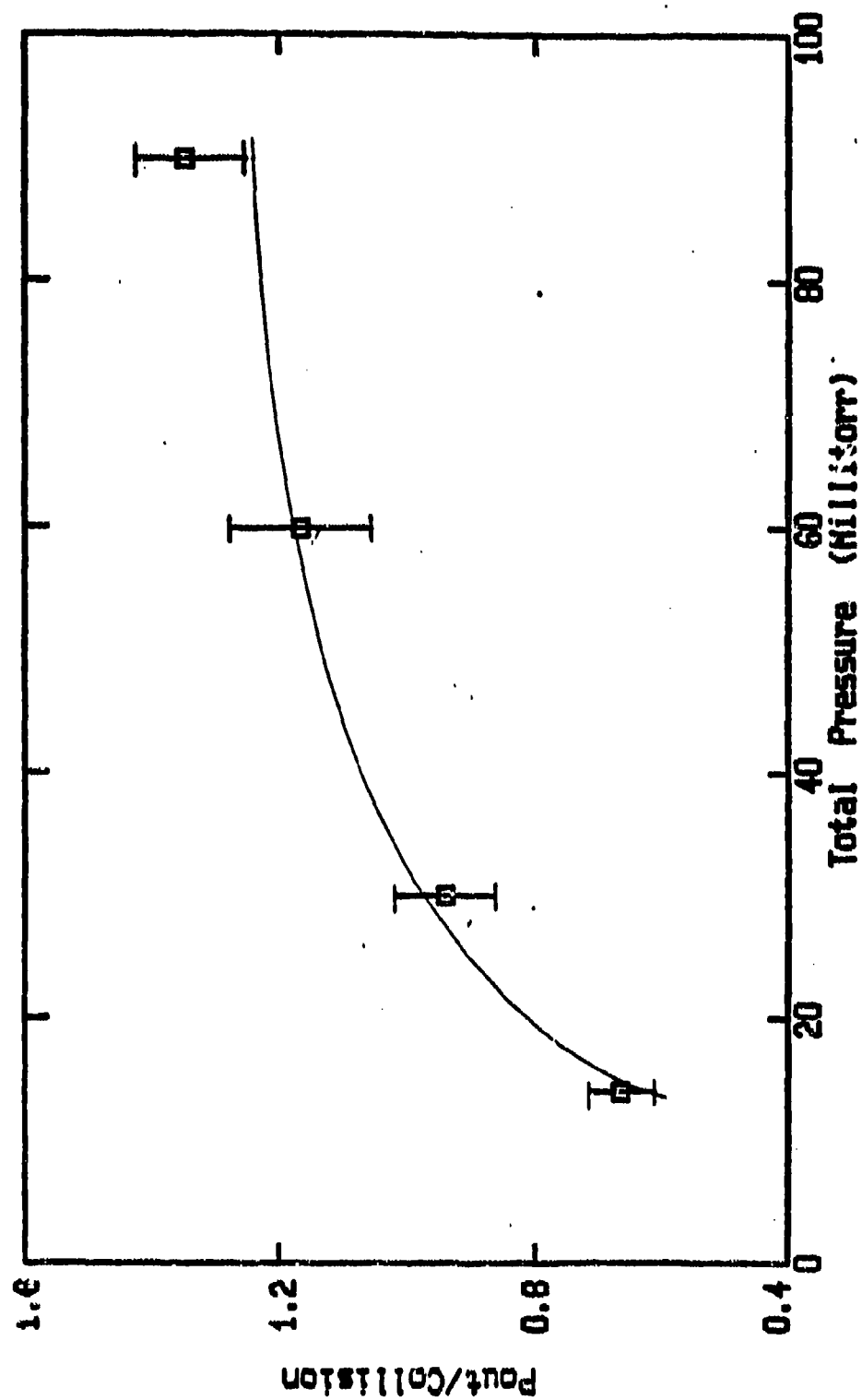
Figure 10. The probability/collision that a molecule in a particular J state of K=3 will decay into the K=3 pool in the 3/4° cell with helium
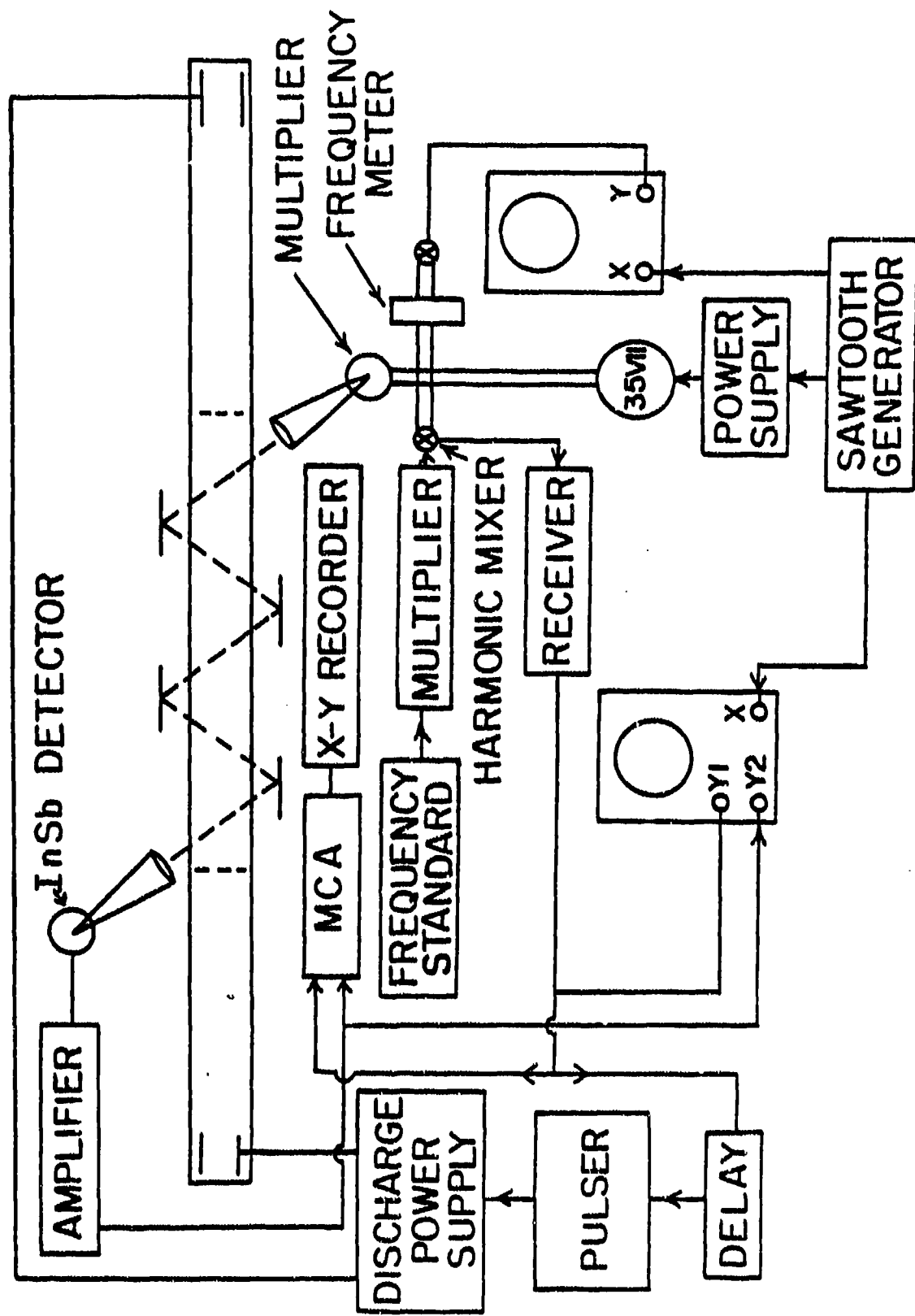
Figure 11. Spectrometer for the study of discharge systems.

Figure 12. The $J=2-3$ transitions of the 01^11, 001, 11^10, and 100 vibrational states of HCN in the laser plasma.

Current = 400 mA

Temp (011/001) = 290 K

Temp (110/100) = 270 K

011

001

110

100

Absorption —>

Frequency (GHz)

264.001 264.021 264.041 264.061 264.081

in Figure 13 both the 100 and 001 are far from thermal equilibrium.
Thus, the $11^1 0$ upper lasing state population vastly exceeds the
$04^0 0$ lower lasing state population. The rapid exchange among
bending modes, which is shown by the thermal equilibrium discussed
above, allows competition effects to substantially enhance the
efficiency of this system.

We have also studied the OCS/CO/CS discharge system.
Figure 14 shows that the principal chemical reaction caused by the
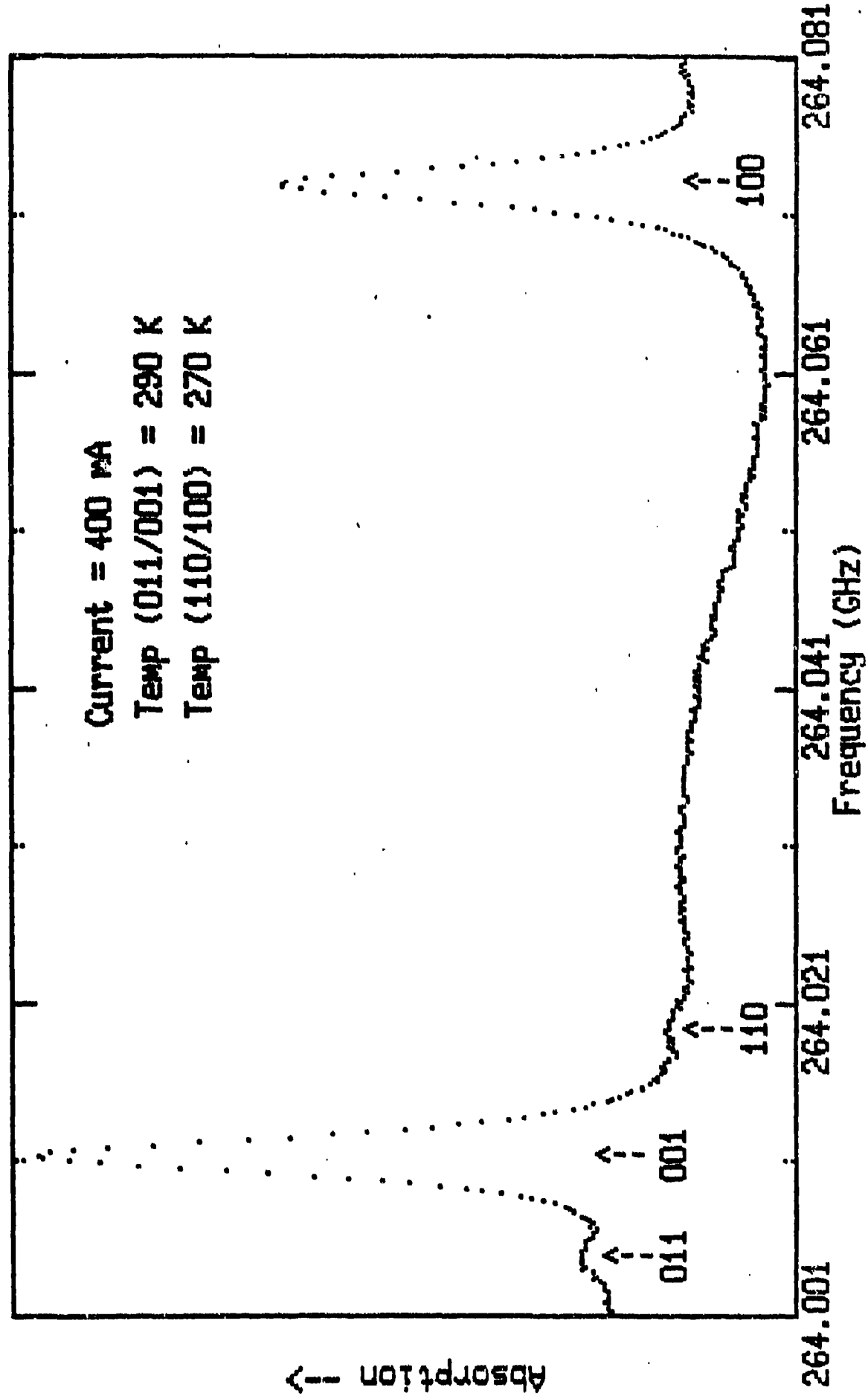discharge is the simple decomposition OCS→CO+S, with secondary re-
actions producing small amounts of CS before the S deposits on the
wall. This model is confirmed by chemical analysis of the wall
deposits which show them to be >95% sulfur and by the observation
that the pressure does not change at the onset of the discharge. In
this system we have modeled the time evolution of the rotational/
translational temperature and the vibrational temperatures. The
time constants associated with the cooling at the end of the dis-
charge pulse can be shown to be in good agreement with those ob-
tained from transport theory. Unlike HCN, we find that the vibra-
tional modes of OCS are not especially "hot". However, CS is
substantially out of equilibrium. Figure 15 shows the decay of
this excess population after the end of the pulse.

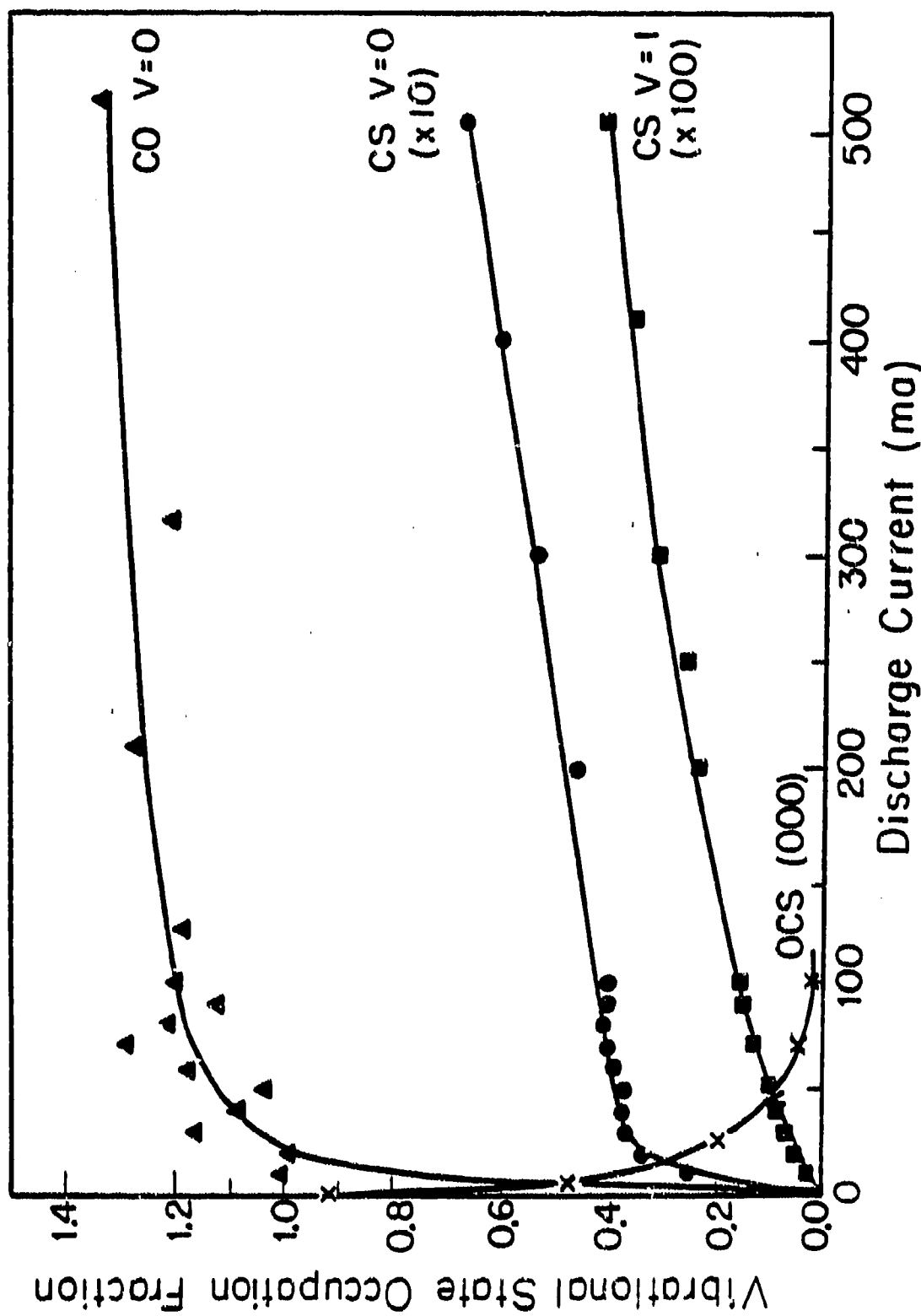Figure 13. Vibrational temperatures of the 100 and 001 vibrational states.
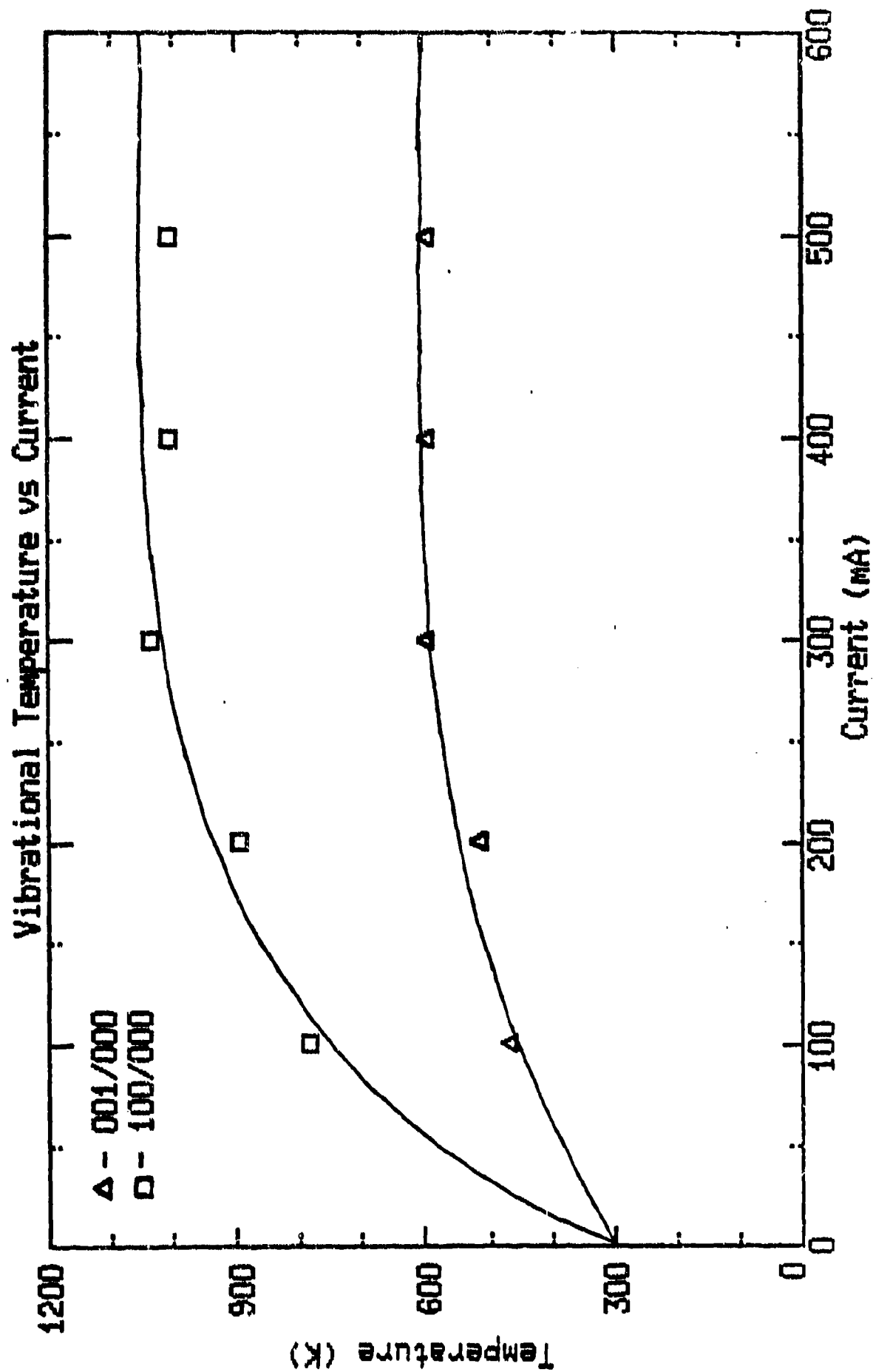
Figure 14. Vibrational state occupation fractions (not normalized) of the major constituents of the OCS/CS/CO discharge system.
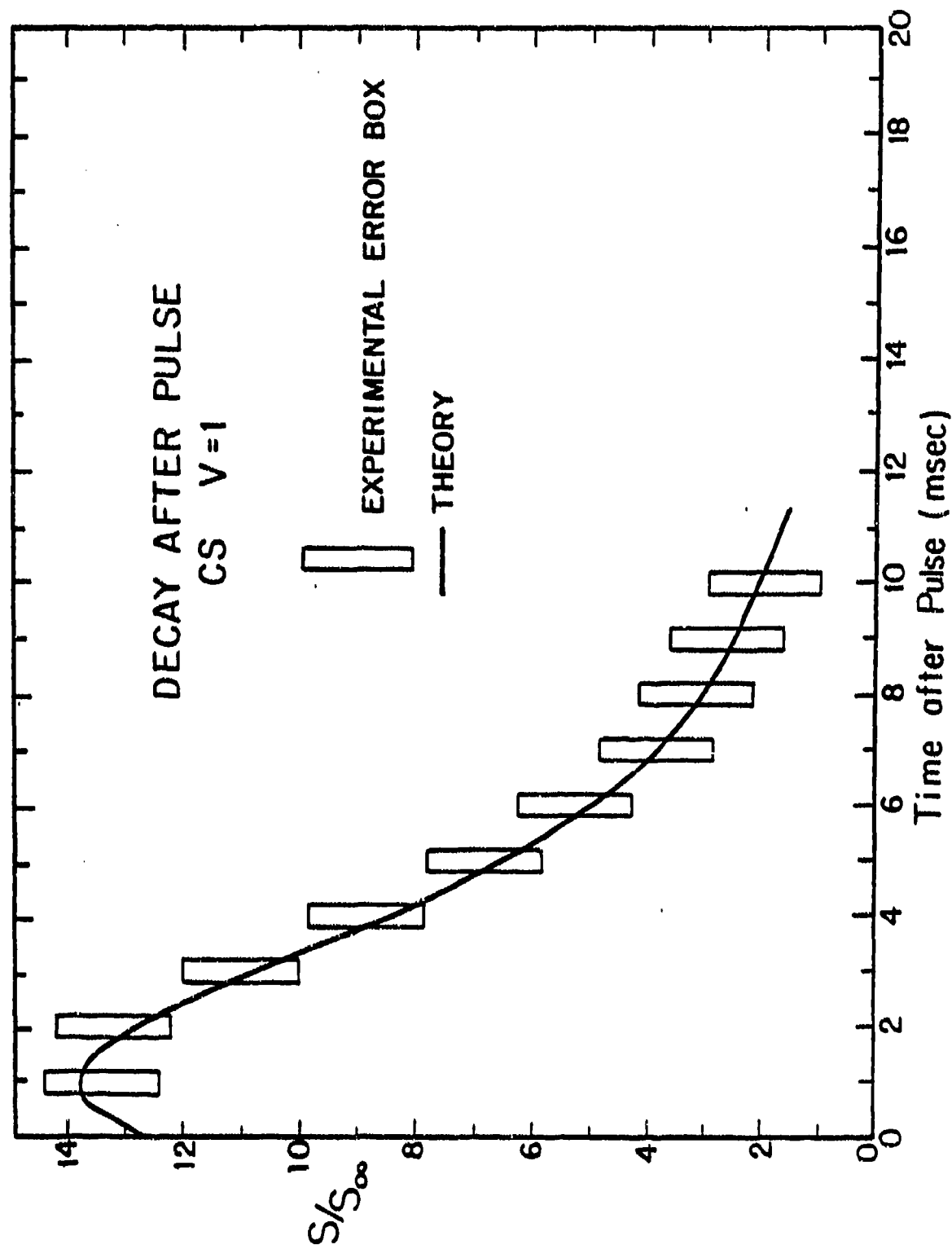
Figure 15. The decay of the vibrational excitation of v=1 CS.

III. Energy Levels and Transition Frequencies of Molecular Species

This is the traditional domain of the spectroscopist and is the foundation for most of the work discussed in this proposal. Work in the MM/SUBMM has historically been difficult and as a result spectroscopic measurements have been minimal in comparison to those in other spectral regions. This is especially true for studies in excited vibrational states and at higher frequencies. Furthermore, we seek to calculate "complete" sets of energy levels and transition frequencies (including their statistical uncertainties) rather than to simply determine the more important spectral constants. This more stringent goal is necessary if it is desired to use this information as an aid to the understanding of atmospheric transmission, molecular lasers, quantum frequency converters, remote sensing data, energy transfer, etc.

This work has many aspects. One of our papers describes extensive new measurments and analyses in the 400-1100 GHz region on water and its major isotopes. The work in this one paper represents almost 40% of the entire microwave data base for this important species. Most of the remaining data is from our earlier work. With this new work, all of the H_2O transitions that make observable contributions to atmospheric absorption in the NMMW spectral region have now been observed. These are shown in Figure 16. Figure 17 shows another result of this work. Here the very accurate diode laser measurements of Worchesky et al. at Harry Diamond Laboratories are combined with our results to calculate the vibrational frequency of D_2O. In conjunction with our studies

Figure 16.   Observed Microwave Transitions in the Ground

State of H_2O (MHz).

Transition	Frequency
6(1,6)— 5(2, 3)	22235.08
3(1,3)— 2(2, 0)	183310.12
10(2,9)— 9(3, 6)	321225.64
5(1,5)— 4(2, 2)	325152.92
4(1,4)— 3(2, 1)	380197.37
10(3,7)—11(2,10)	390134.51
7(5,3)— 6(6, 0)	437346.67
6(4,3)— 5(5, 0)	439150.81
7(5,2)— 6(6, 1)	443018.30
4(2,3)— 3(3, 0)	448001.08
6(4,2)— 5(5, 1)	470888.95
5(3,3)— 4(4, 0)	474689.13
6(2,4)— 7(1, 7)	488491.13
8(6,3)— 7(7, 0)	503568.53
8(6,2)— 7(7, 1)	504482.69
1(1,0)— 1(0, 1)	556936.00
5(3,2)— 4(4, 1)	620700.81
9(7,3)— 8(8, 0)	645766.01
9(7,2)— 8(8, 1)	645905.62
2(1,1)— 2(0, 2)	752033.23
4(2,2)— 3(3, 1)	916171.58
5(2,4)— 4(3, 1)	970315.02
2(0,2)— 1(1, 1)	987926.76

Figure 17. Vibrational Frequency of ν_2 Calculated from Diode Laser Results and the Rotational Analyses of D_2O (cm^{-1}).

Transition	Observed[a] Frequency	Rotational[b] Contribution	Vibrational[c] Frequency
6(6, 0) − 5(5, 1) 6(6, 1) − 5(5, 0)	1035.4343	−142.9397	1178.3740
7(3, 4) − 6(2, 5)	1035.4921	−142.8866	1178.3787
11(3, 9) − 10(2, 8)	1048.7007	−129.6659	1178.3666
12(2,10) − 11(3, 9)	1053.9497	−124.4147	1178.3644
10(1, 9) − 9(2, 8)	1073.2597	−105.1165	1178.3762
5(3, 3) − 4(2, 2)	1079.8632	−98.5161	1178.3793
10(2, 9) − 10(1,10)	1084.6568	−93.7207	1178.3775
9(0, 9) − 8(1, 8)	1085.7458	−92.6323	1178.3781

[a] From Worchesky et al.

[b] Calculated from the analyses of the pure microwave data.

[c] Average calculated vibrational frequency = 1178.3743 cm^{-1}.

of the $^{13}CH_3F$ laser, we made extensive measurements in both the ground and excited vibrational states. An interesting feature of this work is that the absorption spectroscopy measurements in the excited vibrational state give a highly precise value of the FIR laser frequency, which is completely uncomtaminated by pump offset and cavity pulling effects. This technique is an important new method for establishing secondary frequency standards throughout the NMMW. A recent measurement of the $^{13}CH_3F$ laser frequency by Mary Tobin of HDL is in good agreement with our value, but our frequencies are dramatically different than the previously accepted value. We have also investigated the energy level structure and transition frequencies of the new lasing species CHD_2F. We have combined our measurements with the FIR laser frequencies measured by M. S. Tobin and the known CO_2 laser frequencies in a "grand unification" analyses. For this, we used the analysis techniques that we have developed for light asymmetric rotors. The spectral constants that result from this are shown in Figure 18. We have also recently done extensive spectroscopic studies of a number of small fundamental species such as HOOH, NO_2, HNO_3, etc. Although these are geometrically simple species, many of them have especially difficult spectroscopic problems (internal rotation, unpaired electron spin, light asymmetric rotors, etc.). As a result for most of these very fundamental species, prior to our work, their submillimeter absorption frequencies were unknown. Although this work was done primarily under the sponsorship of other agencies, there has recently been considerable interest in their absorption properties in "disturbed" atmospheres. This is a very good example that new

Figure 18. Spectral Constants of CHD_2F (MHz).

Constant	Ground State[a,b]	ν_6 Excited State[a,b]	
A	95207.015(7)	96058.	(10)
B	22405.599(1)	22133.214	(45)
C	21284.478(1)	21255.220	(45)
Δ_J	0.0411659(96)	0.040262	(84)
Δ_{JK}	0.276159 (35)	0.17303	(118)
Δ_K	0.744936 (747)	1.50	(10)
δ_J	0.00195258(66)	−0.000588	(92)
δ_K	0.150917 (234)	−0.052	(21)
$H_{JK} \cdot 10^4$	----	−0.450	(49)
$H_{KJ} \cdot 10^2$	----	0.1592	(95)
$L_{KKJ} \cdot 10^4$	----	0.117	(25)
rms	0.038	0.076 [c]	

[a] The number of places retained is necessary to insure that the constants reproduce the observed data.

[b] The number in the parenthesis is the standard deviation in terms of the last quoted place.

[c] From an analysis of the microwave data alone.

and fundamental measurements and theory on prevasive and wide
spread materials have applications that go far beyond the narrow
applications that we all initially visualize.

Papers That Resulted From This Work

A Spectroscopic Investigation of the OCS Discharge System, William W. Clark and Frank C. De Lucia, J. Chem. Phys. 74, 3139-3147 (1981).

The Millimeter Wave Spectra of NaH and NaD, K.V.L.N. Sastry, Eric Herbst, and Frank C. De Lucia, J. Chem. Phys. 75, 4753-4757 (1981).

Gas Phase Approaches to the Near Millimeter Wave Source Problem, Frank C. De Lucia, Eric Herbst, Michael S. Feld, and W. Happer, IEEE J. of Quantum Electronics QE-17, 2171-2187 (1981).

The Millimeter and Submillimeter Spectrum of CF_2 and Its Production in a DC Glow Discharge, Arthur Charo and Frank C. De Lucia, J. Mol. Spectrosc. 94, 363-368 (1982).

The Production of Large Concentrations of Molecular Ions in the Lengthened Negative Glow Region of a Discharge, Frank C. De Lucia, Eric Herbst, Grant M. Plummer, and Geoffrey A. Blake, J. Chem. Phys. 78, 2312-2316 (1983).

Continuously tunable coherent spectroscopy for the 0.1 to 1.0 THz region, Paul Helminger, James K. Messer, and Frank C. De Lucia, Appl. Phys. Lett. 42, 309-310 (1983).

Millimeterwave Spectroscopic Studies of Collision-induced Energy Transfer Processes in the $^{13}CH_3F$ Laser, William H. Matteson and Frank C. De Lucia, IEEE J. of Quantum Electronics QE-19, 1284-1293 (1983).

The Pure Rotational Spectrum of Water Vapor – A Millimeter, Submillimeter, and Far Infrared Analysis, J.K. Messer, Paul Helminger, and Frank C. De Lucia, International J. of Infrared and Millimeter Waves 4, 505-539 (1983).

Submillimeter Spectroscopy of the Major Isotopes of Water, J.K. Messer, Paul Helminger, and Frank C. De Lucia, accepted for publication.

Spectroscopy of the Energy Levels of the CHD_2F Laser, W.H. Matteson, Frank C. De Lucia, and M. S. Tobin, to be published.

The Submillimeter Spectrum of Methanol, Eric Herbst, Paul Helminger, J. K. Messer, and Frank C. De Lucia, to be published.

A Detailed Diagnostic Study of the Effects of Buffer Gases on Optically Pumped FIR Lasers, W. H. Matteson and Frank C. De Lucia, to be published.

Vibrational Energy Transfer and Equilibria in the HCN FIR Laser,
David D. Skatrud and Frank C. De Lucia, to be published.

Papers Related to This Work But Supported by Other Agencies

A Study of the Rotational-Torsional Spectrum of Hydrogen Peroxide
Between 80 and 700 GHz, Paul Helminger, Wayne C. Bowman, and
Frank C. De Lucia, J. Mol. Spectrosc. $\underline{85}$, 120-130 (1981).

Laboratory Measurements of Millimeter and Submillimeter Rotational
Transitions of NH_2, Arthur Charo, K.V.L.N. Sastry, Eric Herbst,
and Frank C. De Lucia, The Astrophysical J. $\underline{244}$, L111-L112
(1981).

The Higher K_{-1} States of Hydrogen Peroxide, Wayne C. Bowman,
Frank C. De Lucia, and Paul Helminger, J. Mol. Spectrosc. $\underline{87}$,
571-574 (1981).

Millimeter and Submillimeter Spectra of HNO_2(CIS), HNO_2(TRANS),
and HNO_3, Wayne C. Bowman, Frank C. De Lucia, and Paul
Helminger, J. Mol. Spectrosc. $\underline{88}$, 431-433 (1981).

Laboratory Measurements of Millimeter and Submillimeter Transi-
tions of NaH and NaD, K.V.L.N. Sastry, Eric Herbst, and Frank
C. De Lucia, Astrophys. J. Lett. $\underline{248}$, L53-L55 (1981).

Millimeter and Submillimeter Sepctra of HCO^+ and DCO^+, K.V.L.N.
Sastry, Eric Herbst, and Frank C. De Lucia, J. Chem. Phys. $\underline{75}$,
4169-4170 (1981).

Millimeter and Submillimeter Spectra of HN_2^+ and DN_2^+, K.V.L.N.
Sastry, Paul Helminger, Eric Herbst, and Frank C. De Lucia,
Chem. Phys. Lett. $\underline{84}$, 286-287 (1981).

Laboratory Millimeter and Submillimeter Spectra of CO^+, K.V.L.N.
Sastry, Paul Helminger, Eric Herbst, and Frank C. De Lucia,
Astrophys. J. Lett. $\underline{250}$, L91-L92 (1981).

Laboratory Millimeter and Submillimeter Spectrum of CCH, K.V.L.N.
Sastry, Paul Helminger, Eric Herbst, and Frank C. De Lucia,
Astrophys, J. Lett. $\underline{251}$, L119-L120 (1981).

The Millimeter and Submillimeter Spectrum of NO_2: A Study of
Electronic Effects in a Non-singlet Light Asymmetric Rotor,
Wayne C. Bowman and Frank C. De Lucia, J. Chem. Phys. $\underline{77}$,
92-107 (1982).

Millimeter and Submillimeter Spectrum of NO^+, Wayne C. Bowman, Eric Herbst, and Frank C. De Lucia, J. Chem. Phys. <u>77</u>, 4261-4262 (1982).

Laboratory Millimeter and Submillimeter Spectrum of HOC^+, Geoffrey A. Blake, Paul Helminger, Eric Herbst, and Frank C. De Lucia, The Astrophysical J. <u>264</u>, L69-L70 (1983).

The Millimeter and Submillimeter Spectrum of CN in Its First Four Vibrational States, David D. Skatrud and Frank C. De Lucia, J. Mol. Spectrosc. <u>99</u>, 35-46 (1983).

Measurement of the $J = 0 \rightarrow 1$ Rotational Transitions of Three Isotopes of ArD^+, Wayne C. Bowman, Grant M. Plummer, Eric Herbst, and Frank C. De Lucia, J. Chem. Phys. <u>79</u>, 2093-2095 (1983).

Laboratory Measurement of the $J = 2 \rightarrow 3$ Rotational Transition Frequency of $HC^{17}O^+$, Grank M. Plummer, Eric Herbst, and Frank C. De Lucia, Astrophys. J. Lett. <u>270</u>, L99-L100 (1983).

In addition to the above are an approximately equal number of Conference Papers, Abstracts, sections of books, etc. Since these describe essentially the same work, they are not listed here.

Participating Scientific Personnel

1. Frank C. De Lucia, Professor of Physics: Principal Investigator

2. Eric Herbst, Associate Professor of Physics

3. J. K. Messer, Ph.D., Instructor/Research Associate

4. John Kolena, Adjunct Assistant Professor

5. Paul A. Helminger, Professor of Physics, University of South Alabama

6. K.V.L.N. Sastry, Professor of Physics, University of New Brunswick

7. William W. Clark, Research Assistant, Ph.D., Instructor/ Research Associate

8. Arthur Charo, Graduate Student/Post Doctoral Fellow

9. William Matteson, Graduate Student

10. David Skatrud, Graduate Student

11. Grant Plummer, Graduate Student

12. Geoffrey Blake, Graduate Student (Cal Tech)